

EViT: An Eagle Vision Transformer with Bi-Fovea Self-Attention

Yulong Shi¹, Mingwei Sun^{1*}, Yongshuai Wang¹, Rui Wang², Hui Sun², Zengqiang Chen^{1,3}

¹College of Artificial Intelligence, Nankai University, Tianjin 300350, China,

²College of Information Engineering and Automation, Civil Aviation University of China, Tianjin 300300, China,

³Key Laboratory of Intelligent Robotics of Tianjin, Tianjin 300350, China.

ylshi@mail.nankai.edu.cn, smw_sunmingwei@163.com, wang_ys@mail.nankai.edu.cn,
ruiwang@cauc.edu.cn, h-sun@cauc.edu.cn, chenzq@nankai.edu.cn

Abstract

Because of the advancement of deep learning technology, vision transformer has demonstrated competitive performance in various computer vision tasks. Unfortunately, vision transformer still faces some challenges such as high computational complexity and absence of desirable inductive bias. To alleviate these problems, this study proposes a novel Bi-Fovea Self-Attention (BFSA) inspired by the physiological structure and characteristics of bi-fovea vision in eagle eyes. This BFSA can simulate the shallow fovea and deep fovea functions of eagle vision, enabling the network to extract feature representations of targets from coarse to fine, facilitating the interaction of multi-scale feature representations. Additionally, this study designs a Bionic Eagle Vision (BEV) block based on BFSA and CNN. It combines CNN and Vision Transformer, to enhance the network's local and global representation ability for targets. Furthermore, this study develops a unified and efficient general pyramid backbone network family, named Eagle Vision Transformers (EVITs) by stacking the BEV blocks. Experimental results on various computer vision tasks including image classification, object detection, instance segmentation and other transfer learning tasks show that the proposed EVITs perform significantly better than the baselines under similar model sizes, which exhibits faster speed on graphics processing unit compared to other models. Code will be released at <https://github.com/nkusyl>.

Keywords: Bi-Fovea Self-Attention, Bionic Eagle Vision, Eagle Vision Transformer.

1. Introduction

Since 2012, Convolutional Neural Networks (CNNs) have been dominating in various computer vision tasks due to their inherent inductive biases, such as translation invari-

ance and local sensitivity. However, because of the limited receptive field of convolutional kernels, CNNs are difficult to perceive the global information of images, restricting further development and application of CNNs [26, 55]. At the same time, the rapid development of Transformer [47] in Natural Language Processing (NLP) has attracted worldwide attention from computer vision researchers [17, 22]. Compared with the CNNs, Transformers excel at modeling global dependencies of features and capturing extensive contextual information [14, 62]. These two factors are crucial for vision tasks such as image classification [2, 6], object detection [5, 67], and other vision tasks [1, 9, 41].

Inspired by the success of Transformer in NLP, researchers have also attempted to apply transformer to computer vision tasks. Unlike NLP, Vision Transformer (ViT) [11] splits input images into sequences and converts them into sequential data. Self-attention is then utilized to capture global dependencies in images, generating effective feature representations for image classification task, achieving comparable performance to state-of-the-art CNNs. Subsequently, various vision transformer variants [12, 32, 45, 57] have been proposed, to provide new paradigms and solutions for vision tasks, breaking the monopoly of CNNs in vision tasks [11, 31, 32]. Nonetheless, the vision transformer models also face several challenges, including: (1) Compared with CNNs, self-attention in transformer has quadratic computational complexity and memory cost, the problem is especially prominent when dealing with high-resolution images and videos. (2) 2D input images should be converted into 1D input sequences. This process easily leads to networks insufficient ability for modeling spatially localized information and loss of relative positional relationships between features. (3) Because of flexibility of self-attention and complexity of large-scale parameters, vision transformer has no proper inductive bias, making the network tend to overfit the training data.

To alleviate these problems, this paper draws inspiration from biological eagle vision, hope to design a bionic hybrid

*Corresponding author.

backbone network based on convolution and vision transformer. This inspiration did not come from accident. Although the eagle vision and vision transformer come from biological and computer sciences respectively, this paper still finds three similar attributes through analogy as follows. **(1) High resolution and sensitivity:** eagle vision is known for high resolution, wide field of view and keen sensitivity. This allows eagles to quickly capture small prey in vast field. Similarly, the vision transformer allows networks to focus on details in images, thereby capturing critical representations of targets on image classification and other tasks. **(2) Multi-level feature extraction:** eagles process visual information at multiple levels, starting with photoreceptor cells and eventually reach cerebral cortex. Similarly, vision transformer extracts the target features layer by layer through stacking self-attention and Multi-Layer Perceptron (MLP). **(3) Global and local information awareness:** eagle vision can perceive global and local information about surrounding environments, which helps them track preys. The vision transformer also enable networks to establish associations between different regions of images, and obtain the global and local feature representations of targets.

According the above discussions, this paper designs a Bionic Eagle Vision (BEV) block based on unique bi-fovea physiological structure and characteristics of eagle vision. This BEV block consists of Convolutional Positional Embedding (CPE), Bi-Fovea Self-Attention (BFSA) and Convolutional Feed-Forward Network (CFFN). Based on hierarchical design concepts [20, 49], this paper forms a general vision backbone network framework by stacking multiple BEV blocks, called Eagle Vision Transformer (EViT). Furthermore, this paper scales the depth and width of the EViT, expanding it into a backbone network family comprising four variants: EViT-Tiny, EViT-Small, EViT-Base and EViT-Large, for enhanced applicability across various visual tasks. To best of our knowledge, this is the first work to combine eagle vision with vision transformer on large-scale datasets such as ImageNet [37] and is also the first study to propose a generalized family of vision backbone networks based on eagle vision.

The main contributions of the paper are as follows.

- Benefiting from biological eagle vision, this paper proposes a novel Bi-Fovea Self-Attention (BFSA) for simulating the deep-fovea and shallow-fovea functions of eagle vision, especially to enhance the network's ability to capture fine-grained representations of targets.
- On the foundation of BFSA, this paper introduces BEV block. This BEV block combines the advantages of CNNs and Vision Transformers, aiming to incorporate proper inductive bias in Transformers, reducing network depth and memory cost.
- This paper proposes a unified and efficient general pyramid backbone network family, EViT. It has

good generalization and superiority in image classification, object detection, instance segmentation and other transfer learning tasks, especially in achieving a better trade-off between computational accuracy and efficiency.

The remainder of this paper is structured as follows. Section 2 summarizes the related work of this paper in biological eagle vision and vision transformer, respectively. Section 3 is the main part of the paper that describes the design ideas and details of EViT. Section 4 shows the experimental results of EViT on various vision tasks. Section 5 concludes this paper.

2. Related Work

2.1. Eagle Vision Mechanism

It is widely known that eagles possess an excellent natural visual system, with keen observation of the environment [33]. Figure 1 shows the physiological structure and photoreceptor cell density distribution of the bi-fovea in eagle eyes. From Figure 1, in terms of physiological structure, the eagle eyes have two distinct fovea, namely, deep fovea and shallow fovea. The deep fovea, located in center of retina and has high density of photoreceptor cells. These cells are important to improve the visual resolution of eagle eyes, allowing eagles to recognize prey at long distances and capture them [13]. The shallow fovea is in peripheral area of retina, has relatively low density of photoreceptor cells, but can provide a wider field of view [3].

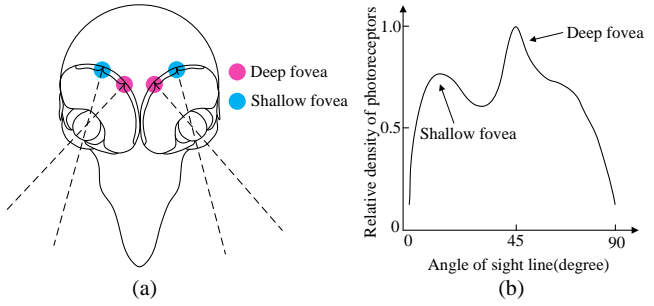


Figure 1. (a) shows the physiological structure of the bi-fovea in eagle eyes; figure (b) shows the density distribution of photoreceptor cells in bi-fovea.

Although one eye of eagles cannot use both deep fovea and shallow fovea for imaging, but it's worth noting that the eagle two eyes can collaborate, alternating between the deep fovea and shallow fovea [3]. For example, when an eagle looks ahead, the deep fovea of one eye is used for fine target recognition, at same time the other eye's shallow fovea can be used to perceive the surrounding environment. This paper refers the above-mentioned eagle vision characteristic as interaction mechanism. Based on this observation, this paper proposes a BFSA module for simulating deep fovea and shallow fovea of eagle vision, enabling

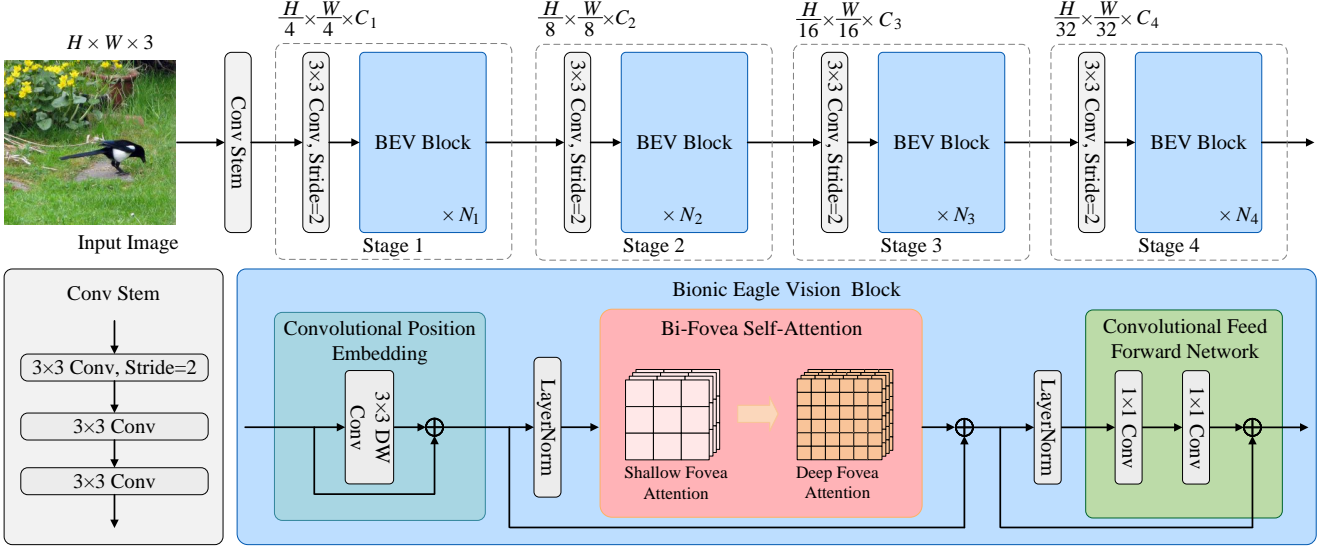


Figure 2. Illustration of the EViT. EViT is composed of a convolutional stem, multiple 3×3 convolution layers with stride 2 and BEV blocks. A BEV block consists of CPE, BFSA and CFFN.

deep learning network to capture the feature representation of targets from coarse to fine, which is important for vision tasks.

2.2. Transformers for Vision

Transformer was originally designed for machine translation task [4, 10], many transformer variants have made great progress in various natural language processing tasks [4, 10, 51]. ViT [11] is a pioneering work that introduces transformer into vision tasks, it only consists of transformer encoder and patch embedding. Compared with CNNs, the biggest difference is that vision transformer use self-attention as an alternative to convolution for global context modeling. After ViT, researchers have proposed a series of improving methods [18, 32, 58], which drive the rapid development of transformer in computer vision. In training phase, DeiT [42] leverages knowledge distillation idea, introduces distillation tokens into the input sequence of transformer encoder, to guide the learning process of the transformer. CvT [52] introduces convolutional token embedding and convolutional projection into transformer framework to obtain local context information and global relative positional relationships of feature sequences. Subsequent work [8, 48, 64] incorporates convolution into the early stages of the transformer to improve the stability of model training. CMT [15] and PVT [49] are hybrid models of CNN and Transformer. To mitigate the memory cost of multi-head self-attention, they use depth-wise convolution to reduce the spatial size of the feature token before the projection operation. Inspired by the recent transformer models, this paper proposes a novel and effective hybrid model of CNN and Transformer by using designed BFSA module and BEV block, expecting that the integration of the

two model frameworks can bring more performance breakthroughs in vision tasks.

3. Approach

3.1. Overall Architecture

In order to take advantages of CNNs and Transformers, alleviate the problems of high computational complexity and lack of desirable inductive bias in vision transformer models. This paper proposes a novel CNNs and Transformers hybrid network architecture inspired by eagle vision properties, called Eagle Vision Transformer (EViT). The overall pipeline of EViT is illustrated in Figure 2. Given an input image with the size of $H \times W \times 3$, it first feed into a convolutional stem to obtain the low-level feature representations. This convolutional stem follows the proposal of previous works [21, 25], employing three successive 3×3 convolution layers at early stage for stabilizing the training process of the network, where, the first convolution layer with stride 2. Then, these low-level representations are processed through a series of 3×3 convolution layers and BEV blocks to generate hierarchical representations of targets, which is important for vision dense prediction tasks. It is worth illustrating that, these 3×3 convolutional layers are used for patch embedding, so that the spatial size of feature maps halved and dimensions doubled before entering the next stage. As a backbone network for multiple vision tasks, this paper follows standard pyramid four-stage design [20, 49]. Each stage has similar architecture, which contains a 3×3 convolution layer with stride 2 and N_i BEV blocks. The difference is the resolution of the output features for stage1-4 are reduced by factors of 4, 8, 16 and 32, and the corresponding channel dimensions are increased to

C_1 , C_2 , C_3 and C_4 . Finally, in image classification task, this paper uses 1×1 convolution projection, average pooling layer and fully connected layer as classifier to output the predictions.

3.2. Bionic Eagle Vision Block

The BEV block achieves complements of convolution and vision transformer. A BEV block consists of three key components: Convolutional Positional Embedding (CPE), Bi-Fovea Self-Attention (BFSA) and Convolutional Feed-Forward Network (CFFN). The complete mathematical definition of BEV block is shown in Equation 1 to Equation 3.

$$\mathbf{X} = \text{CPE}(\mathbf{X}_{in}) + \mathbf{X}_{in} \quad (1)$$

$$\mathbf{Y} = \text{BFSA}(\text{LN}(\mathbf{X})) + \mathbf{X} \quad (2)$$

$$\mathbf{Z} = \text{CFFN}(\text{LN}(\mathbf{Y})) + \mathbf{Y} \quad (3)$$

Where, the LN is denoted as LayerNorm function, which is used to normalize the feature tensors. Taking stage 1 as an example, when token tensor $\mathbf{X}_{in} \in R^{H \times W \times C}$ is input into the BEV block, this paper first uses CPE to introduce feature location information into all tokens. Compared with Absolute Position Embedding (APE) [32] and Relative Position Embedding (RPE) [38], CPE can more flexibly learn arbitrary resolution feature position information through zero padding of the convolution function. Then, this paper employs BFSA to extract and interactive fusion the global and fine-grained feature representations among tokens. The details of BFSA will be elaborated in the following subsection. Finally, this paper uses two 1×1 convolutional layers as CFFN to further enhance the feature representation of each token.

3.3. Bi-Fovea Self-Attention

Figure 1 shows the physiological structure and photoreceptor cell density distribution of bi-fovea in eagle eyes. Relatively speaking, the shallow fovea of eagle eye can achieve coarse-grained surroundings perception, and the deep fovea can achieve fine-grained prey recognition. Taking inspiration from this, this paper aims to build a similar module as bi-fovea in eagle eyes, which can extract the global and fine feature representation of images. This leads to the proposal of Bi-Fovea Self-Attention (BFSA). The illustration of this BFSA module is shown in Figure 3, where this BFSA consists of two Token Interaction Fusion (TIF) module, a Shallow Fovea Attention (SFA) and a Deep Fovea Attention (DFA).

Token Interaction Fusion. In original Multi-Head Self-Attention (MHSA), the token tensor $\mathbf{X}'_{in} \in R^{H \times W \times C}$ is first projected into Query $\mathbf{Q} \in R^{N \times D}$, Key $\mathbf{K} \in R^{N \times D}$ and Value $\mathbf{V} \in R^{N \times D}$, where N and D are the length and dimension of the input token sequence, respectively. To mitigate the computational overhead of MHSA, this paper first

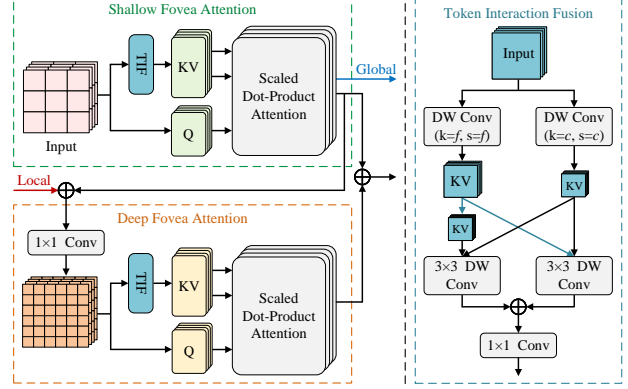


Figure 3. Illustration of the BFSA. The BFSA consists of two Token Interaction Fusion (TIF) module, a Shallow Fovea Attention (SFA) and a Deep Fovea Attention (DFA)

designs a Token Interaction Fusion (TIF) module based on depth-wise convolution and 1×1 convolution. It used to reduce the spatial size of \mathbf{K} and \mathbf{V} inputs before the projection operation. The structure of this TIF is shown in Figure 3, where the cyan arrows denote the down-sampling of the feature representation by using 3×3 depth-wise convolution with stride 2 and padding 1. It has two parameters, c and f , which are used to control the reduced size of feature tokens. The TIF also enables the extraction and interaction of multi-scale feature tokens, which is particularly important for vision dense prediction tasks.

Shallow Fovea Attention. In SFA, this paper takes $\mathbf{Q} = \text{Linear}(\mathbf{X}'_{in})$, $\mathbf{K}' = \text{Linear}(\text{TIF}(\mathbf{X}'_{in}))$ and $\mathbf{V}' = \text{Linear}(\text{TIF}(\mathbf{X}'_{in}))$ as inputs and uses them to model the global relationship between each token, yielding attention scores. The compact matrix form of the SFA is defined as shown in Equation 4 to Equation 6.

$$\text{SFA}(\mathbf{X}'_{in}) = \text{Concat}(\mathbf{head}_0, \mathbf{head}_1, \dots, \mathbf{head}_h) \mathbf{W}^o \quad (4)$$

$$\mathbf{head}_i = \text{Attention}(\mathbf{Q}_i, \mathbf{K}'_i, \mathbf{V}'_i) \quad (5)$$

$$\text{Attention}(\mathbf{Q}, \mathbf{K}', \mathbf{V}') = \text{softmax}\left(\frac{\mathbf{Q}\mathbf{K}'^T}{\sqrt{D}}\right)\mathbf{V}' \quad (6)$$

where $\mathbf{head}_i \in R^{N \times \frac{D}{h}}$ is the output of the i^{th} attention head, the weight matrix $\mathbf{W}^o \in R^{N \times \frac{D}{h}}$ is used to compose all heads.

Deep Fovea Attention. In DFA, the mathematical definitions of DFA and SFA are the same, the only difference between them is that the inputs are different. In order to incorporate proper inductive bias in BFSA and enhance its local feature representation ability, this paper uses two 1×1 convolutions and a 3×3 deep convolution to design a Local Information Awareness (LIA) module via residual bottleneck connection [20]. This LIA combines the local connectivity of CNN and the global context of vision transformer in a complementary manner, encouraging the DFA to learn the structural information and local relationships within each

Output size	Layer Name	EViT-Tiny	EViT-Small	EViT-Base	EViT-Large
112 × 112	Conv Stem	$3 \times 3, 24, \text{stride } 2$ $[3 \times 3, 20] \times 2$	$3 \times 3, 28, \text{stride } 2$ $[3 \times 3, 24] \times 2$	$3 \times 3, 32, \text{stride } 2$ $[3 \times 3, 28] \times 2$	$3 \times 3, 32, \text{stride } 2$ $[3 \times 3, 32] \times 2$
56 × 56	Patch Embedding	$2 \times 2, 48, \text{stride } 2$	$2 \times 2, 56, \text{stride } 2$	$2 \times 2, 64, \text{stride } 2$	$2 \times 2, 64, \text{stride } 2$
Stage 1	BEV block	$\begin{bmatrix} H_1=1, c_1=8 \\ f_1=4, r_1=3 \end{bmatrix} \times 2$	$\begin{bmatrix} H_1=1, c_1=8 \\ f_1=4, r_1=3.5 \end{bmatrix} \times 2$	$\begin{bmatrix} H_1=1, c_1=8 \\ f_1=4, r_1=3.5 \end{bmatrix} \times 3$	$\begin{bmatrix} H_1=1, c_1=8 \\ f_1=4, r_1=4 \end{bmatrix} \times 4$
28 × 28	Patch Embedding	$2 \times 2, 96, \text{stride } 2$	$2 \times 2, 112, \text{stride } 2$	$2 \times 2, 128, \text{stride } 2$	$2 \times 2, 128, \text{stride } 2$
Stage 2	BEV block	$\begin{bmatrix} H_2=2, c_2=4 \\ f_2=2, r_2=3 \end{bmatrix} \times 2$	$\begin{bmatrix} H_2=2, c_2=4 \\ f_2=2, r_2=3.5 \end{bmatrix} \times 2$	$\begin{bmatrix} H_2=2, c_2=4 \\ f_2=2, r_2=3.5 \end{bmatrix} \times 3$	$\begin{bmatrix} H_2=2, c_2=4 \\ f_2=2, r_2=4 \end{bmatrix} \times 4$
14 × 14	Patch Embedding	$2 \times 2, 192, \text{stride } 2$	$2 \times 2, 224, \text{stride } 2$	$2 \times 2, 256, \text{stride } 2$	$2 \times 2, 256, \text{stride } 2$
Stage 3	BEV block	$\begin{bmatrix} H_3=4, c_3=2 \\ f_3=1, r_3=3 \end{bmatrix} \times 2$	$\begin{bmatrix} H_3=4, c_3=2 \\ f_3=1, r_3=3.5 \end{bmatrix} \times 6$	$\begin{bmatrix} H_3=4, c_3=2 \\ f_3=1, r_3=3.5 \end{bmatrix} \times 8$	$\begin{bmatrix} H_3=4, c_3=2 \\ f_3=1, r_3=4 \end{bmatrix} \times 10$
7 × 7	Patch Embedding	$2 \times 2, 384, \text{stride } 2$	$2 \times 2, 448, \text{stride } 2$	$2 \times 2, 512, \text{stride } 2$	$2 \times 2, 512, \text{stride } 2$
Stage 4	BEV block	$\begin{bmatrix} H_4=8, c_4=1 \\ f_4=1, r_4=3 \end{bmatrix} \times 2$	$\begin{bmatrix} H_4=8, c_4=1 \\ f_4=1, r_4=3.5 \end{bmatrix} \times 2$	$\begin{bmatrix} H_4=8, c_4=1 \\ f_4=1, r_4=3.5 \end{bmatrix} \times 3$	$\begin{bmatrix} H_4=8, c_4=1 \\ f_4=1, r_4=4 \end{bmatrix} \times 4$
1 × 1	Projection			1 × 1, 1280	
1 × 1	Classifier			Fully Connected Layer, 1000	
Params		12.67 M	24.10 M	42.47 M	55.71 M
FLOPs		1.71 G	3.53 G	6.23 G	8.16 G

Table 1. The four architectural variants of EViTs for ImageNet classification. H_i denotes the number of attention heads in DFA and SFA of stage i . c_i and f_i are used to control the reduced size of feature tokens of stage i . r_i denotes the expansion ratio in CFFN of stage i .

feature token. It is worth to note that, this paper takes the output of SFA and the $\mathbf{X}'_{in} \in R^{H \times W \times C}$ as the input of LIA. The complete mathematical definition of LIA module is shown in Equation 7.

$$\text{LIA}(\mathbf{X}) = \text{Conv}(\text{DWConv}(\text{Conv}(\mathbf{X})) + \text{Conv}(\mathbf{X})) \quad (7)$$

where $\mathbf{X} = \text{Concat}(\mathbf{X}'_{in} + \text{SFA}(\mathbf{X}'_{in}))$, activation and normalization functions are omitted. We uses the outputs of SFA and LIA as input to DFA. The input of this DFA is shown in Equation 8.

$$\mathbf{X}''_{in} = \text{Conv}(\text{SFA}(\mathbf{X}'_{in}) + \text{LIA}(\mathbf{X}'_{in} + \text{SFA}(\mathbf{X}'_{in}))) \quad (8)$$

Finally, this paper combines the outputs of SFA and DFA, and feeds them to the next layer. The process is shown in Equation 9.

$$\mathbf{Out} = \text{Concat}(\text{SFA}(\mathbf{X}'_{in}) + \text{DFA}(\mathbf{X}''_{in})) \quad (9)$$

In summary, The SFA and DFA simulate the shallow fovea and deep fovea function of eagle eyes. This paper uses SFA to model global dependencies between feature tokens and uses DFA to capture fine-grained feature representations of targets. This LIA establishes a link between the SFA and the DFA and introduces an appropriate inductive bias for the BFSA. It implements the complementation and fusion of the global dependency of transformer and the local representation of convolution in an elegant way.

3.4. Architecture Variants of EViT

This paper uses BEV block as basic building block, and proposes a novel general vision pyramid backbone network family, called EViTs. In order to facilitate comparison with other backbone networks under similar model size and computational complexity, this paper designs four variants, EViT-Tiny, EViT-Small, EViT-Base and EViT-Large. The structural details of EViTs are shown in Table 1. These variants follow the dominant four-stage pyramid structure design, with each stage having different number of BEV blocks and hidden feature dimensions to adapt to the needs of various vision tasks. This paper uses a 3×3 convolution with a stride 2 for patch embedding, and to connect these different stages, so that the spatial size of feature maps halved and dimensions doubled before entering the next stage. Therefore, each stage can output feature maps of four different sizes to obtain rich hierarchical feature representations of targets. In order to facilitate showing the implementation details of the four variants, this paper unifies their input image resolutions in Table 1, all of those are 224^2 . Specially, during the training process, the input image resolutions of EViT-Tiny, EViT-Small, EViT-Base and EViT-Large are 160^2 , 192^2 , 224^2 , and 256^2 respectively.

4. Experiments

To evaluate the effectiveness of EViT, this paper applies EViT to a series of mainstream computer vision

tasks, including ImageNet-1K [37] classification (Sec. 4.1), COCO 2017 [29] object detection and instance segmentation (Sec. 4.2), and other transfer learning tasks (Sec. 4.3). Specifically, this paper first trains the EViT from scratch on ImageNet-1K dataset to implement image classification, and obtains the pre-training parameters of EViT. After that, this paper fine-tunes the pre-training parameters of EViT on COCO 2017 and other vision datasets respectively by transfer learning, which is used to validate the performance of EViT in object detection, instance segmentation, and other downstream vision tasks. In addition to them, this study conducted the ablation experiments on EViT in (Sec. 4.4), which was used to validate the effectiveness of the BFSA and TIF.

4.1. Image Classification on ImageNet-1k

Settings. This paper first evaluates the proposed models (EViT-Tiny, EViT-Small, EViT-Base and EViT-Large) in ImageNet-1K [37] dataset. The ImageNet-1K dataset contains 1000 classes with total of about 1.33M images, where the training dataset has about 1.28M images and the validation dataset has 50K images. For the sake of fairness, this paper follows the same training strategy as DeiT [42] and PVT [49] to compare with other methods. Specifically, this paper selects AdamW as the network parameter optimizer and trains all models for 300 epochs. The weight decay is 0.05. The initial learning rate is 0.001 and follows cosine decay. This paper employs the same data augmentations as DeiT [42], including random flipping, random cropping, random erasing [66], CutMix [60], Mixup [61] and label smoothing [39]. During the training process, the input image resolutions of these four network variants are 160^2 , 192^2 , 224^2 , and 256^2 respectively.

Results. In this section, we compare EViTs with popular efficient CNN and ViT models, and report the experimental results in Table 2. The results show that EViTs obtain the best accuracy and speed trade-off compared to other methods under similar model parameters. In specifically, EViT-Tiny and EViT-Small implement better classification performance with smaller input image resolution and fewer model parameters, achieving 79.8% and 82.1%, respectively. Compared to Swin-S [32], NestT-Small [65], CvT-21 [52], and ViL-Medium [63], EViT-Base has better performance and less computational cost. Specifically, EViT-Base achieves 84.1% Top-1 accuracy with 5.0G FLOPs. It improves the performance by 0.8% over the four mentioned methods, and reduces nearly 1.5 to 5 times of computational complexity at the same time. At larger model scales, EViT-Large still has significant competitive advantages over other existing methods. In particular, for fair comparison with other methods, this paper specifically organizes two experiments on EViT-Large in image classification at 224^2 and 256^2 image sizes. At the same settings, EViT-Large ob-

Model	Resolution	FLOPs (G)	Params (M)	Top-1 Acc (%)
ResNet-18 [20]	224^2	1.8	11.7	69.8
RegNetY-1.6G [36]	224^2	1.6	11.2	78.0
PVT-T [49]	224^2	1.9	13.2	75.1
PVTv2-b1 [50]	224^2	2.1	13.1	78.7
PyramidTNT-Ti [16]	224^2	0.6	10.6	75.2
CoaT-Lite Mini [54]	224^2	2.0	11.0	78.9
EfficientViT-M5 [30]	224^2	0.5	12.4	77.1
LocalViT-PVT [27]	224^2	4.8	13.5	78.2
EViT-Tiny	160^2	0.8	12.6	79.8
ResNet-50 [20]	224^2	4.1	25.6	79.0
DeiT-S [42]	224^2	4.6	22.1	79.8
PVT-S [49]	224^2	3.7	24.5	79.8
T2T-14 [59]	224^2	5.2	20.0	81.5
TNT-S [18]	224^2	5.2	23.8	81.3
PVT-S [49]	224^2	3.8	24.5	79.8
LocalViT-S [27]	224^2	4.6	22.4	80.8
Swin-T [32]	224^2	4.5	28.3	81.3
CvT-13 [52]	224^2	4.5	20.0	81.6
EViT-Small	192^2	2.6	24.1	82.1
ResNet-101 [20]	224^2	7.9	45.0	77.4
RegNetY-8G [36]	224^2	8.0	39.2	79.9
PVT-M [49]	224^2	6.4	44.2	81.2
Swin-S [32]	224^2	8.7	49.6	83.3
NestT-Small [65]	224^2	10.4	38	83.3
CvT-21 [52]	384^2	24.9	31.5	83.3
MViT-B [12]	224^2	7.8	37	81.0
CViT-18 [6]	224^2	9.0	43	82.5
ViL-Medium [63]	224^2	9.1	39.7	83.3
EViT-Base	224^2	6.2	42.5	84.1
ResNet-152 [20]	224^2	11.6	60.0	82.0
T2T-24 [59]	224^2	14.1	64	82.3
TNT-B [18]	224^2	14.1	65.6	82.8
PVT-L [49]	224^2	9.8	61.4	81.7
PVT v2-B4 [50]	224^2	10.1	62.6	83.6
CaiT-S36 [43]	224^2	13.9	68	83.3
NestT-Base [65]	224^2	17.9	68	83.8
EViT-Large	224^2	8.1	55.7	84.5
EViT-Large	256^2	10.8	55.7	85.1

Table 2. ImageNet-1K classification results of EViTs. This paper groups similar CNNs and Transformers together based on model parameters and classification performance. The proposed EViTs consistently outperform other methods and with less computational cost.

tained 2.8% and 1.2% performance gains compared to PVT-L [49] and CaiT-S36 [43]. When the input image size is set to 256^2 , the model parameters of EViT-Large is only 59.3M, but obtains a classification performance of 85.1%. After the above experiments, this paper observes that the competitive advantages of EViT are low computational complexity and scalability. In terms of low computational complexity, this paper introduces convolutional operations into the EViTs, and designs a TIF module based on convolution, which is used to reduce the size of feature tokens in BFSA and decrease the computational complexity of EViT. In terms of scalability, EViT can be better scaled to smaller or larger models dependent on task requirements.

4.2. Object Detection and Instance Segmentation

Settings. This paper conducts object detection and instance segmentation experiments for EViTs on COCO 2017 [29] dataset. The COCO 2017 dataset contains 80 classes, 118k training images, 5k validation images and 20k test-dev images. This paper uses two representative frameworks, Reti-

Backbone	RetinaNet							Mask R-CNN						
	Params (M)	<i>mAP</i>	AP_{50}	AP_{75}	AP_S	AP_M	AP_L	Params (M)	mAP^b	AP_{50}^b	AP_{75}^b	mAP^m	AP_{50}^m	AP_{75}^m
ResNet-50 [20]	37.7	36.3	55.3	38.6	19.3	40.0	48.8	44.2	38.0	58.6	41.4	34.4	55.1	36.7
Swin-T [32]	38.5	41.5	62.1	44.2	25.1	44.9	55.5	47.8	42.2	64.6	46.2	39.1	61.6	42.0
DAT-T [53]	38.0	42.8	64.4	45.2	28.0	45.8	57.8	48.0	44.4	67.6	48.5	40.4	64.2	43.1
ResT-Base [64]	40.5	42.0	63.2	44.8	29.1	45.3	53.3	49.8	41.6	64.9	45.1	38.7	61.6	41.4
PVT-T [49]	34.2	40.4	61.3	43.0	25.0	42.9	55.7	44.1	40.4	62.9	43.8	37.8	60.1	40.3
PVTv2-B2 [50]	35.1	44.6	65.6	47.6	27.4	48.8	58.6	45.0	45.3	67.1	49.6	41.2	64.2	44.4
EViT-Small	31.9	45.2	66.1	48.8	28.4	49.2	59.7	41.7	46.6	68.3	50.2	42.3	65.5	45.3
ResNet-101 [20]	56.7	38.5	57.8	41.2	21.4	42.6	51.1	63.2	40.4	41.1	44.2	36.4	57.7	38.8
Swin-S [32]	59.8	44.5	65.7	47.5	27.4	48.0	59.9	69.1	44.8	66.6	48.9	40.9	63.4	44.2
DAT-S [53]	60.0	45.7	67.7	48.5	30.5	49.3	61.3	69.0	47.1	69.9	51.5	42.5	66.7	45.4
PVT-M [49]	53.9	41.9	63.1	44.3	25.0	44.9	57.6	63.9	42.0	64.4	45.6	39.0	61.6	42.1
PVTv2-B3 [50]	55.0	45.9	66.8	49.3	28.6	49.8	61.4	64.9	47.0	68.1	51.7	42.5	65.7	45.7
EViT-Base	50.4	46.8	68.3	50.7	30.9	51.2	62.3	60.1	47.9	69.2	52.5	43.5	66.4	46.6

Table 3. Performance comparison of object detection (left group) and instance segmentation (right group) on the COCO 2017 val dataset. All models are used as a visual backbone and then plugged into the RetinaNet [28] and Mask R-CNN [19] frameworks.

naNet [28] and Mask R-CNN [19], respectively, to evaluate the performance of EViT in object detection and instance segmentation tasks. The EViT is used as the vision backbone and is then plugged into RetinaNet and Mask R-CNN frameworks. Before training, this paper uses the pre-trained weights on ImageNet-1k to initialize the EViT backbone, and other layers are randomly initialized. To be fair, this paper follows the same settings as MMDection [7]: the short side of the input image is resized to 800, and the long side is at most 1333; the optimizer is selected to AdamW, with an initial learning rate of 0.0001 and weight decay of 0.05; the training schedule is 1×12 epochs.

Results. Table 3 shows the performance comparison between EViT and other backbone networks for object detection and instance segmentation on COCO 2017 val dataset. For RetinaNet framework, this paper uses mean Average Precision (*mAP*), Average Precision at 50% and 75% IoU thresholds (AP_{50} , AP_{75}), and for three object sizes precision (small, medium, and large (AP_S , AP_M , and AP_L)) as the evaluation metrics for model performance. From the results, it can be seen the EViTs has significant competitive advantages compared with other methods. In particular, the average accuracy of EViT-Small and EViT-Base has at least 8% higher than ResNet-50 and ResNet-101, and also higher than the advanced PVTv2-B2 and PVTv2-B3 with 0.6% and 0.9%. For Mask R-CNN framework, this paper uses bounding box Average Precision (AP_b) and mask Average Precision (AP_m) at different IoU thresholds (50%, 75%). From the results, EViT-Small and EViT-Base also significantly outperform the ResNet. Specifically, in mAP^b and mAP^m metrics, EViT-Small is ahead of PVTv2-B2 2.5%, 2.0% and EViT-Base is ahead of PVTv2-B3 1.6%, 1.2% respectively.

4.3. Other vision transfer learning tasks

Settings. In this section, this paper has conducted other transfer learning experiments on various vision datasets to

evaluate the performance of EViTs in different downstream vision tasks. These vision tasks consist of different application scenes, including fine-grained visual classification (Standford Cars [23], Oxford-102 Followers [34] and Oxford-IIIT-Pets [35]), long-tailed classification (iNaturalist18 [46], iNaturalist19 [46]) and superordinate classification (CIFAR10 [24], CIFAR100 [24]). The details of above datasets are listed in Table 4. For fairness, this paper follows the same settings as CMT [15]. Before training, this paper uses the pre-trained weights on ImageNet-1k to initialize the EViT backbone, and other layers are randomly initialized.

dataset	application	classes	train data	val data
Standford Cars [23]	fine-grained	196	8133	8041
Oxford-102 Flowers [34]	visual	102	2040	6149
Oxford-IIIT-Pets [35]	classification	37	3680	3669
iNaturalist18 [46]	long-tailed	8142	437513	24426
iNaturalist19 [46]	classification	1010	265240	3003
CIFAR10 [24]	superordinate	10	50000	10000
CIFAR100 [24]	classification	100	50000	10000

Table 4. Details of used vision datasets. The table includes the number of classes, training images and test images of these datasets

Results. Table 5 shows the performance comparison between EViT and other backbone networks on these above vision tasks. As can be seen from the results, EViTs exhibit extremely competitive performance. In particular, EViT achieves comparable performance to EfficientNet-B7 with the least computational cost and ahead of other convolution and transformer models in classification accuracy. This demonstrates the superiority of the EViTs designed in this paper based on eagle bi-foveal vision.

4.4. Ablation Study

Settings. In this section, this paper conducts ablation experiments for the proposed EViTs by using ImageNet-1K image classification dataset, which is used to validate the ef-

Model	Params (M)	FLOPs (G)	Cars	Flowers	Pets	iNaturalist18	iNaturalist19	CIFAR10	CIFAR100
Grafit ResNet-50 [44]	25.6	4.1	92.5%	98.2%	-%	-%	75.9%	-%	-%
EfficientNet-B5 \uparrow_{456} [40]	28.0	10.3	93.9%	98.5%	94.9%	-%	-%	98.7%	91.1%
CeiT-S [58]	24.2	4.8	94.1%	98.6%	94.9%	73.3%	78.9%	99.1%	90.8%
TNT-S \uparrow_{384} [18]	23.8	5.2	-%	98.8%	94.7%	-%	-%	98.7%	90.1%
ViTAE-S [56]	23.6	5.6	91.4%	97.8%	94.2%	-%	76.0%	98.8%	90.8%
EViT-Small	24.1	2.6	94.3%	98.7%	95.1%	73.4%	79.1%	99.1%	91.4%
TNT-b \uparrow_{384} [18]	65.6	14.1	-%	99.0%	95.0%	-%	-%	99.1%	91.1%
EfficientNet-B7 \uparrow_{600} [40]	64.0	37.2	94.7%	98.8%	95.4%	-%	-%	98.9%	91.7%
ViT-B/16 \uparrow_{384} [11]	85.8	17.6	-%	89.5%	93.8%	-%	-%	98.1%	87.1%
DeiT-B [42]	85.8	17.3	92.1%	98.4%	-%	73.2%	77.7%	99.1%	90.8%
EViT-Base	42.5	6.2	94.8%	98.8%	95.3%	73.7%	79.6%	99.3%	91.7%

Table 5. Performance comparison between EViT and other backbone networks on fine-grained visual classification task, long-tailed classification task and superordinate classification task.

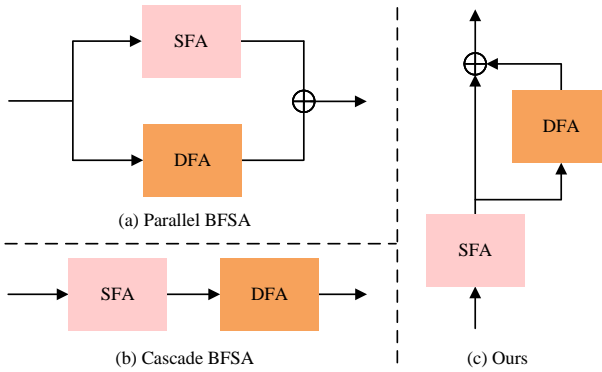


Figure 4. The three types of BFSA connections.

fectiveness of BFSA and TIF. EViT-Base is considered for use in this ablation study. Specifically, the input image size is set to 224^2 , and the depth and width of the EViT-Base are kept constant as set in Table 1.

Structural analysis of the BFSA. This paper a major contribution is designed a Bi-Fovea Self-Attention (BFSA) by using the interaction mechanism of eagle vision. It achieves excellent performance in various vision tasks, such as image classification, object detection, and instance segmentation. This largely depends on the unique design concept and structure of the BFSA. Figure 4(c) shows the unique connection structure of Shallow Fovea Attention (SFA) and Deep Fovea Attention (DFA) in BFSA by simplification. As can be seen from Figure 4, the BFSA does not simply connect SFA and DFA in parallel or cascade, it is more like a combination of the two. Therefore, this paper first analyzes the structure of the BFSA, which is used to demonstrate the effectiveness of this unique structure. In the implementation details, this paper designs Parallel BFSA and Cascade BFSA by parallel connection and cascade connection between SFA and DFA, respectively, which are used to compare with the original BFSA proposed in this paper. Table 6 shows the performance comparison of the BFSA for the three connections. As can be seen from the results, although BFSA is slightly higher than the Parallel BFSA and Cascade BFSA in computational complexity and parameters, but it has significant advantages in performance. In

Method	FLOPs (G)	Params (M)	Top-1 Acc (%)
Parallel BFSA	5.7	40.0	81.6
Cascade BFSA	5.9	41.3	82.3
BFSA (Ours)	6.2	42.5	84.1
CSR	6.1	39.9	83.7
TIF	6.2	42.5	84.1

Table 6. Results of the ablation experiments for BFSA and TIF.

particular, BFSA is higher than parallel BFSA by 2.5% and cascade BFSA by 1.2% in image classification accuracy, respectively. It can be shown that the unique structural design of the BFSA is extremely effective.

Effectiveness analysis of TIF. In subsection 3.3, this paper designs a Token Interaction Fusion (TIF) module for reducing the feature tokens sizes. This TIF not only can alleviate the computational burden of self-attention, but also can facilitate the interaction and fusion of multi-scale feature tokens. To demonstrate the effectiveness of TIF, this paper conducted an ablation experiment for the TIF. Specifically, this paper follows PVT by using a convolution to reduce the spatial size of feature tokens. For ease of analysis, this paper refers the method as Convolutional Spatial Reduction (CSR). Table 6 shows the performance comparison between TIF and CSR, with the results it can be seen that TIF achieves 0.4% performance improvement with only 2.6M parameter cost and negligible computational complexity. It can be shown that the TIF is effective.

5. Conclusion

This paper proposes a novel Bi-Fovea Self-Attention (BFSA) to enable the network to extract object feature representations from coarse to fine, and facilitate the interaction of multi-scale feature representations. The core idea of BFSA is to simulate the eagle-eye bi-fovea vision interaction mechanism, which can help the network to model the global feature dependencies of images and extract fine-grained representations of objects at the same time. Furthermore, this paper designs a Bionic Eagle Vision (BEV) block based on BFSA. This BEV implements the comple-

mentary of transformer and convolution, and used as basic block to build Eagle Vision Transformers (EViT). Extensive experiments show that EViT can be effectively used as a backbone for various downstream tasks, and has excellent performance in image classification, object detection and instance segmentation tasks, which are competitive with other Transformers.

Acknowledgement

This work was supported by the National Natural Science Foundation of China (Grant No. 62073177 and 61973175).

References

- [1] Anurag Arnab, Mostafa Dehghani, Georg Heigold, Chen Sun, Mario Lučić, and Cordelia Schmid. Vivit: A video vision transformer. In *Proceedings of the IEEE/CVF International Conference on Computer Vision*, pages 6836–6846, 2021. 1
- [2] Srinadh Bhojanapalli, Ayan Chakrabarti, Daniel Glasner, Daliang Li, Thomas Unterthiner, and Andreas Veit. Understanding robustness of transformers for image classification. In *Proceedings of the IEEE/CVF International Conference on Computer Vision*, pages 10231–10241, 2021. 1
- [3] Andreas Bringmann. Structure and function of the bird fovea. *Anatomia, Histologia, Embryologia*, 48(3):177–200, 2019. 2
- [4] Tom Brown, Benjamin Mann, Nick Ryder, Melanie Subbiah, Jared D Kaplan, Prafulla Dhariwal, Arvind Neelakantan, Pranav Shyam, Girish Sastry, Amanda Askell, et al. Language models are few-shot learners. *Advances in Neural Information Processing Systems*, 33:1877–1901, 2020. 3
- [5] Nicolas Carion, Francisco Massa, Gabriel Synnaeve, Nicolas Usunier, Alexander Kirillov, and Sergey Zagoruyko. End-to-end object detection with transformers. In *European Conference on Computer Vision*, pages 213–229. Springer, 2020. 1
- [6] Chun-Fu Richard Chen, Quanfu Fan, and Rameswar Panda. Crossvit: Cross-attention multi-scale vision transformer for image classification. In *Proceedings of the IEEE/CVF International Conference on Computer Vision*, pages 357–366, 2021. 1, 6
- [7] Kai Chen, Jiaqi Wang, Jiangmiao Pang, Yuhang Cao, Yu Xiong, Xiaoxiao Li, Shuyang Sun, Wansen Feng, Ziwei Liu, Jiarui Xu, et al. Mmdetection: Open mmlab detection toolbox and benchmark. *arXiv preprint arXiv:1906.07155*, 2019. 7
- [8] Qiang Chen, Qiman Wu, Jian Wang, Qinghao Hu, Tao Hu, Errui Ding, Jian Cheng, and Jingdong Wang. Mixformer: Mixing features across windows and dimensions. In *Proceedings of the IEEE/CVF Conference on Computer Vision and Pattern Recognition*, pages 5249–5259, 2022. 3
- [9] Peifang Deng, Kejie Xu, and Hong Huang. When cnns meet vision transformer: A joint framework for remote sensing scene classification. *IEEE Geoscience and Remote Sensing Letters*, 19:1–5, 2021. 1
- [10] Jacob Devlin, Ming-Wei Chang, Kenton Lee, and Kristina Toutanova. Bert: Pre-training of deep bidirectional transformers for language understanding. *arXiv preprint arXiv:1810.04805*, 2018. 3
- [11] Alexey Dosovitskiy, Lucas Beyer, Alexander Kolesnikov, Dirk Weissenborn, Xiaohua Zhai, Thomas Unterthiner, Mostafa Dehghani, Matthias Minderer, Georg Heigold, Sylvain Gelly, et al. An image is worth 16x16 words: Transformers for image recognition at scale. *arXiv preprint arXiv:2010.11929*, 2020. 1, 3, 8
- [12] Haoqi Fan, Bo Xiong, Karttikeya Mangalam, Yanghao Li, Zhicheng Yan, Jitendra Malik, and Christoph Feichtenhofer. Multiscale vision transformers. In *Proceedings of the IEEE/CVF International Conference on Computer Vision*, pages 6824–6835, 2021. 1, 6
- [13] Julio González-Martín-Moro, JL Hernández-Verdejo, and A Clement-Corral. The visual system of diurnal raptors: updated review. *Archivos de la Sociedad Española de Oftalmología (English Edition)*, 92(5):225–232, 2017. 2
- [14] Jiaqi Gu, Hyoukjun Kwon, Dilin Wang, Wei Ye, Meng Li, Yu-Hsin Chen, Liangzhen Lai, Vikas Chandra, and David Z Pan. Multi-scale high-resolution vision transformer for semantic segmentation. In *Proceedings of the IEEE/CVF Conference on Computer Vision and Pattern Recognition*, pages 12094–12103, 2022. 1
- [15] Jianyuan Guo, Kai Han, Han Wu, Yehui Tang, Xinghao Chen, Yunhe Wang, and Chang Xu. Cmt: Convolutional neural networks meet vision transformers. In *Proceedings of the IEEE/CVF Conference on Computer Vision and Pattern Recognition*, pages 12175–12185, 2022. 3, 7
- [16] Kai Han, Jianyuan Guo, Yehui Tang, and Yunhe Wang. Pyramidtn: Improved transformer-in-transformer baselines with pyramid architecture. *arXiv preprint arXiv:2201.00978*, 2022. 6
- [17] Kai Han, Yunhe Wang, Hanting Chen, Xinghao Chen, Jianyuan Guo, Zhenhua Liu, Yehui Tang, An Xiao, Chunjing Xu, Yixing Xu, et al. A survey on vision transformer. *IEEE Transactions on Pattern Analysis and Machine Intelligence*, 45(1):87–110, 2022. 1
- [18] Kai Han, An Xiao, Enhua Wu, Jianyuan Guo, Chunjing Xu, and Yunhe Wang. Transformer in transformer. *Advances in Neural Information Processing Systems*, 34:15908–15919, 2021. 3, 6, 8
- [19] Kaiming He, Georgia Gkioxari, Piotr Dollár, and Ross Girshick. Mask r-cnn. In *Proceedings of the IEEE International Conference on Computer Vision*, pages 2961–2969, 2017. 7
- [20] Kaiming He, Xiangyu Zhang, Shaoqing Ren, and Jian Sun. Deep residual learning for image recognition. In *Proceedings of the IEEE Conference on Computer Vision and Pattern Recognition*, pages 770–778, 2016. 2, 3, 4, 6, 7
- [21] Huaiibo Huang, Xiaoqiang Zhou, Jie Cao, Ran He, and Tie-niu Tan. Vision transformer with super token sampling. In *Proceedings of the IEEE/CVF Conference on Computer Vision and Pattern Recognition*, pages 22690–22699, 2023. 3
- [22] Salman Khan, Muzammal Naseer, Munawar Hayat, Syed Waqas Zamir, Fahad Shahbaz Khan, and Mubarak Shah. Transformers in vision: A survey. *ACM Computing Surveys (CSUR)*, 54(10s):1–41, 2022. 1

[23] Jonathan Krause, Michael Stark, Jia Deng, and Li Fei-Fei. 3d object representations for fine-grained categorization. In *Proceedings of the IEEE International Conference on Computer Vision Workshops*, pages 554–561, 2013. 7

[24] Alex Krizhevsky, Geoffrey Hinton, et al. Learning multiple layers of features from tiny images. 2009. 7

[25] Youngwan Lee, Jonghee Kim, Jeffrey Willette, and Sung Ju Hwang. Mpvit: Multi-path vision transformer for dense prediction. In *Proceedings of the IEEE/CVF Conference on Computer Vision and Pattern Recognition*, pages 7287–7296, 2022. 3

[26] Wenshuo Li, Hanting Chen, Jianyuan Guo, Ziyang Zhang, and Yunhe Wang. Brain-inspired multilayer perceptron with spiking neurons. In *Proceedings of the IEEE/CVF Conference on Computer Vision and Pattern Recognition*, pages 783–793, 2022. 1

[27] Yawei Li, Kai Zhang, Jiezhang Cao, Radu Timofte, and Luc Van Gool. Localvit: Bringing locality to vision transformers. *arXiv preprint arXiv:2104.05707*, 2021. 6

[28] Tsung-Yi Lin, Priya Goyal, Ross Girshick, Kaiming He, and Piotr Dollár. Focal loss for dense object detection. In *Proceedings of the IEEE International Conference on Computer Vision*, pages 2980–2988, 2017. 7

[29] Tsung-Yi Lin, Michael Maire, Serge Belongie, James Hays, Pietro Perona, Deva Ramanan, Piotr Dollár, and C Lawrence Zitnick. Microsoft coco: Common objects in context. In *Computer Vision–ECCV 2014: 13th European Conference, Zurich, Switzerland, September 6–12, 2014, Proceedings, Part V 13*, pages 740–755. Springer, 2014. 6

[30] Xinyu Liu, Houwen Peng, Ningxin Zheng, Yuqing Yang, Han Hu, and Yixuan Yuan. Efficientvit: Memory efficient vision transformer with cascaded group attention. In *Proceedings of the IEEE/CVF Conference on Computer Vision and Pattern Recognition*, pages 14420–14430, 2023. 6

[31] Yang Liu, Yao Zhang, Yixin Wang, Feng Hou, Jin Yuan, Jiang Tian, Yang Zhang, Zhongchao Shi, Jianping Fan, and Zhiqiang He. A survey of visual transformers. *IEEE Transactions on Neural Networks and Learning Systems*, 2023. 1

[32] Ze Liu, Yutong Lin, Yue Cao, Han Hu, Yixuan Wei, Zheng Zhang, Stephen Lin, and Baining Guo. Swin transformer: Hierarchical vision transformer using shifted windows. In *Proceedings of the IEEE/CVF International Conference on Computer Vision*, pages 10012–10022, 2021. 1, 3, 4, 6, 7

[33] Mindaugas Mitkus, Simon Potier, Graham R Martin, Olivier Duriez, and Almut Kelber. Raptor vision. In *Oxford Research Encyclopedia of Neuroscience*, 2018. 2

[34] Maria-Elena Nilsback and Andrew Zisserman. Automated flower classification over a large number of classes. In *2008 Sixth Indian Conference on Computer Vision, Graphics & Image processing*, pages 722–729. IEEE, 2008. 7

[35] Omkar M Parkhi, Andrea Vedaldi, Andrew Zisserman, and CV Jawahar. Cats and dogs. In *2012 IEEE Conference on Computer Vision and Pattern Recognition*, pages 3498–3505. IEEE, 2012. 7

[36] Ilija Radosavovic, Raj Prateek Kosaraju, Ross Girshick, Kaiming He, and Piotr Dollár. Designing network design spaces. In *Proceedings of the IEEE/CVF Conference on Computer Vision and Pattern Recognition*, pages 10428–10436, 2020. 6

[37] Olga Russakovsky, Jia Deng, Hao Su, Jonathan Krause, Sanjeev Satheesh, Sean Ma, Zhiheng Huang, Andrej Karpathy, Aditya Khosla, Michael Bernstein, et al. Imagenet large scale visual recognition challenge. *International Journal of Computer Vision*, 115:211–252, 2015. 2, 6

[38] Peter Shaw, Jakob Uszkoreit, and Ashish Vaswani. Self-attention with relative position representations. In *Proceedings of the 2018 Conference of the North American Chapter of the Association for Computational Linguistics: Human Language Technologies, Volume 2 (Short Papers)*, pages 464–468, 2018. 4

[39] Christian Szegedy, Vincent Vanhoucke, Sergey Ioffe, Jon Shlens, and Zbigniew Wojna. Rethinking the inception architecture for computer vision. In *Proceedings of the IEEE Conference on Computer Vision and Pattern Recognition*, pages 2818–2826, 2016. 6

[40] Mingxing Tan and Quoc Le. Efficientnet: Rethinking model scaling for convolutional neural networks. In *International Conference on Machine Learning*, pages 6105–6114. PMLR, 2019. 8

[41] Yucheng Tang, Dong Yang, Wenqi Li, Holger R Roth, Bennett Landman, Daguang Xu, Vishwesh Nath, and Ali Hatamizadeh. Self-supervised pre-training of swin transformers for 3d medical image analysis. In *Proceedings of the IEEE/CVF Conference on Computer Vision and Pattern Recognition*, pages 20730–20740, 2022. 1

[42] Hugo Touvron, Matthieu Cord, Matthijs Douze, Francisco Massa, Alexandre Sablayrolles, and Hervé Jégou. Training data-efficient image transformers & distillation through attention. In *International Conference on Machine Learning*, pages 10347–10357. PMLR, 2021. 3, 6, 8

[43] Hugo Touvron, Matthieu Cord, Alexandre Sablayrolles, Gabriel Synnaeve, and Hervé Jégou. Going deeper with image transformers. In *Proceedings of the IEEE/CVF International Conference on Computer Vision*, pages 32–42, 2021. 6

[44] Hugo Touvron, Alexandre Sablayrolles, Matthijs Douze, Matthieu Cord, and Hervé Jégou. Grafit: Learning fine-grained image representations with coarse labels. In *Proceedings of the IEEE/CVF International Conference on Computer Vision*, pages 874–884, 2021. 8

[45] Zhengzhong Tu, Hossein Talebi, Han Zhang, Feng Yang, Peyman Milanfar, Alan Bovik, and Yinxiao Li. Maxvit: Multi-axis vision transformer. In *European Conference on Computer Vision*, pages 459–479. Springer, 2022. 1

[46] Grant Van Horn, Oisin Mac Aodha, Yang Song, Alexander Shepard, Hartwig Adam, Pietro Perona, and Serge Belongie. The inaturalist challenge 2017 dataset. *arXiv preprint arXiv:1707.06642*, 1(2):4, 2017. 7

[47] Ashish Vaswani, Noam Shazeer, Niki Parmar, Jakob Uszkoreit, Llion Jones, Aidan N Gomez, Łukasz Kaiser, and Illia Polosukhin. Attention is all you need. *Advances in Neural Information Processing Systems*, 30, 2017. 1

[48] Cong Wang, Hongmin Xu, Xiong Zhang, Li Wang, Zhitong Zheng, and Haifeng Liu. Convolutional embedding makes

hierarchical vision transformer stronger. In *European Conference on Computer Vision*, pages 739–756. Springer, 2022. 3

[49] Wenhai Wang, Enze Xie, Xiang Li, Deng-Ping Fan, Kaitao Song, Ding Liang, Tong Lu, Ping Luo, and Ling Shao. Pyramid vision transformer: A versatile backbone for dense prediction without convolutions. In *Proceedings of the IEEE/CVF International Conference on Computer Vision*, pages 568–578, 2021. 2, 3, 6, 7

[50] Wenhai Wang, Enze Xie, Xiang Li, Deng-Ping Fan, Kaitao Song, Ding Liang, Tong Lu, Ping Luo, and Ling Shao. Pvt v2: Improved baselines with pyramid vision transformer. *Computational Visual Media*, 8(3):415–424, 2022. 6, 7

[51] Thomas Wolf, Lysandre Debut, Victor Sanh, Julien Chaumond, Clement Delangue, Anthony Moi, Pierrick Cistac, Tim Rault, Rémi Louf, Morgan Funtowicz, et al. Transformers: State-of-the-art natural language processing. In *Proceedings of the 2020 Conference on Empirical Methods in Natural Language Processing: System Demonstrations*, pages 38–45, 2020. 3

[52] Haiping Wu, Bin Xiao, Noel Codella, Mengchen Liu, Xiyang Dai, Lu Yuan, and Lei Zhang. Cvt: Introducing convolutions to vision transformers. In *Proceedings of the IEEE/CVF International Conference on Computer Vision*, pages 22–31, 2021. 3, 6

[53] Zhuofan Xia, Xuran Pan, Shiji Song, Li Erran Li, and Gao Huang. Vision transformer with deformable attention. In *Proceedings of the IEEE/CVF Conference on Computer Vision and Pattern Recognition*, pages 4794–4803, 2022. 7

[54] Weijian Xu, Yifan Xu, Tyler Chang, and Zhuowen Tu. Co-scale conv-attentional image transformers. In *Proceedings of the IEEE/CVF International Conference on Computer Vision*, pages 9981–9990, 2021. 6

[55] Yifan Xu, Huapeng Wei, Minxuan Lin, Yingying Deng, Kekai Sheng, Mengdan Zhang, Fan Tang, Weiming Dong, Feiyue Huang, and Changsheng Xu. Transformers in computational visual media: A survey. *Computational Visual Media*, 8:33–62, 2022. 1

[56] Yufei Xu, Qiming Zhang, Jing Zhang, and Dacheng Tao. Vitae: Vision transformer advanced by exploring intrinsic inductive bias. *Advances in Neural Information Processing Systems*, 34:28522–28535, 2021. 8

[57] Ting Yao, Yehao Li, Yingwei Pan, Yu Wang, Xiao-Ping Zhang, and Tao Mei. Dual vision transformer. *IEEE Transactions on Pattern Analysis and Machine Intelligence*, 2023. 1

[58] Kun Yuan, Shaopeng Guo, Ziwei Liu, Aojun Zhou, Fengwei Yu, and Wei Wu. Incorporating convolution designs into visual transformers. In *Proceedings of the IEEE/CVF International Conference on Computer Vision*, pages 579–588, 2021. 3, 8

[59] Li Yuan, Yunpeng Chen, Tao Wang, Weihao Yu, Yujun Shi, Zi-Hang Jiang, Francis EH Tay, Jiashi Feng, and Shuicheng Yan. Tokens-to-token vit: Training vision transformers from scratch on imagenet. In *Proceedings of the IEEE/CVF International Conference on Computer Vision*, pages 558–567, 2021. 6

[60] Sangdoo Yun, Dongyoon Han, Seong Joon Oh, Sanghyuk Chun, Junsuk Choe, and Youngjoon Yoo. Cutmix: Regularization strategy to train strong classifiers with localizable features. In *Proceedings of the IEEE/CVF International Conference on Computer Vision*, pages 6023–6032, 2019. 6

[61] Hongyi Zhang, Moustapha Cisse, Yann N Dauphin, and David Lopez-Paz. mixup: Beyond empirical risk minimization. *arXiv preprint arXiv:1710.09412*, 2017. 6

[62] Jiangning Zhang, Xiangtai Li, Yabiao Wang, Chengjie Wang, Yibo Yang, Yong Liu, and Dacheng Tao. Eatformer: Improving vision transformer inspired by evolutionary algorithm. *arXiv preprint arXiv:2206.09325*, 2022. 1

[63] Pengchuan Zhang, Xiyang Dai, Jianwei Yang, Bin Xiao, Lu Yuan, Lei Zhang, and Jianfeng Gao. Multi-scale vision longformer: A new vision transformer for high-resolution image encoding. In *Proceedings of the IEEE/CVF International Conference on Computer Vision*, pages 2998–3008, 2021. 6

[64] Qinglong Zhang and Yu-Bin Yang. Rest: An efficient transformer for visual recognition. *Advances in Neural Information Processing Systems*, 34:15475–15485, 2021. 3, 7

[65] Zizhao Zhang, Han Zhang, Long Zhao, Ting Chen, Sercan Ö Arik, and Tomas Pfister. Nested hierarchical transformer: Towards accurate, data-efficient and interpretable visual understanding. In *Proceedings of the AAAI Conference on Artificial Intelligence*, volume 36, pages 3417–3425, 2022. 6

[66] Zhun Zhong, Liang Zheng, Guoliang Kang, Shaozi Li, and Yi Yang. Random erasing data augmentation. In *Proceedings of the AAAI Conference on Artificial Intelligence*, volume 34, pages 13001–13008, 2020. 6

[67] Xizhou Zhu, Weijie Su, Lewei Lu, Bin Li, Xiaogang Wang, and Jifeng Dai. Deformable detr: Deformable transformers for end-to-end object detection. *arXiv preprint arXiv:2010.04159*, 2020. 1